

Immunocytochemical Analysis of Uukuniemi Virus Budding Compartments: Role of the Intermediate Compartment and the Golgi Stack in Virus Maturation

JUSSI JÄNTTI,^{1,2} PEKKA HILDÉN,¹ HANNE RÖNKÄ,¹ VIRPI MÄKIRANTA,¹ SIRKKA KERÄNEN,²
AND ESA KUISMANEN^{1*}

Department of Biosciences, Division of Biochemistry, Genetics and Cell Biology Programme, University of Helsinki Biocenter, Helsinki University, Helsinki,¹ and VTT Biotechnology and Food Research, Espoo,² Finland

Received 12 July 1996/Accepted 18 October 1996

Previous studies have suggested that Uukuniemi virus, a bunyavirus, matures at the membranes of the Golgi complex. In this study we have employed immunocytochemical techniques to analyze in detail the budding compartment(s) of the virus. Electron microscopy of infected BHK-21 cells showed that virus particles are found in the cisternae throughout the Golgi stack. Within the cisternae, the virus particles were located preferentially in the dilated rims. This would suggest that virus budding may begin at or before the *cis* Golgi membranes. The virus budding compartment was studied further by immunoelectron microscopy with a pre-Golgi intermediate compartment marker, p58, and a Golgi stack marker protein, mannosidase II (ManII). Virus particles and budding virus were detected in ManII-positive Golgi stack membranes and, interestingly, in both juxtannuclear and peripheral p58-positive elements of the intermediate compartment. In cells incubated at 15°C the nucleocapsid and virus envelope proteins were seen to accumulate in the intermediate compartment. Immunoelectron microscopy demonstrated that at 15°C the nucleocapsid is associated with membranes that show a characteristic distribution and tubulo-vesicular morphology of the pre-Golgi intermediate compartment. These membranes contained virus particles in the lumen. The results indicate that the first site of formation of Uukuniemi virus particles is the pre-Golgi intermediate compartment and that virus budding continues in the Golgi stack. The results raise questions about the intracellular transport pathway of the virus particles, which are 100 to 120 nm in diameter and are therefore too large to be transported in the 60-nm-diameter vesicles postulated to function in the intra-Golgi transport. The distribution of the virus in the Golgi stack may imply that the cisternae themselves have a role in the vectorial transport of virus particles.

Based on electron microscopy and double-label immunofluorescence, it has been suggested that Uukuniemi virus, a bunyavirus, matures by budding at intracellular smooth membranes of the Golgi complex (13, 14, 16). This mode of maturation is a general feature among bunyaviruses (25). Targeting and retention of the Uukuniemi virus envelope glycoproteins G1 and G2, as well as binding of the nucleocapsid to the Golgi-associated membranes, are likely to be important factors in the determination of the intracellular site of virus budding. The envelope glycoproteins of Uukuniemi virus are synthesized as a precursor protein (43) which is processed to G1 and G2 during the translation and translocation in the endoplasmic reticulum (ER) (14). The glycoproteins are then transported to the Golgi complex where they accumulate (13), apparently due to a retention signal in the cytosolic portion of the G1 glycoprotein (26, 34). The glycoproteins are transported with different kinetics to the site of virus maturation (14, 16), presumably due to different folding kinetics of G1 and G2 (30). In mature virus particles the glycoproteins exist as homodimers (33), which would suggest that homodimeric G1 and G2 interact in the formation of characteristic envelope-spike complexes. Whether this interaction occurs during virus budding or at an earlier step in the glycoprotein biosynthesis is not known.

Immunocytochemical studies with Uukuniemi virus-infected cells have shown that the nucleocapsid is also targeted to Golgi membranes (14). In virus-infected BHK-21 cells the nucleocapsid is concentrated in the Golgi region in parallel with the accumulation of glycoproteins at Golgi membranes (15). Interestingly, the association of the nucleocapsid with the Golgi correlates with the vacuolization of the Golgi stack (15). By immunoelectron microscopy an apparent association of the nucleocapsid with the cytoplasmic face of the Golgi cisternae and Golgi-associated vacuoles is observed (16). The association of the nucleocapsid with the Golgi membranes occurs even in the presence of monensin, although the normal budding of Uukuniemi virus is inhibited (16). It is evident that during virus maturation the nucleocapsid has to bind to the cytoplasmic domains of one or both of the virus glycoproteins because Uukuniemi virus particles do not contain a matrix protein mediating the interaction between the envelope and the nucleocapsid. Previous immunoprecipitation experiments suggest that both glycoproteins are needed for the nucleocapsid association (14).

Although the role of the Golgi complex in the virus budding is clearly established, the boundaries of the budding compartment(s) in the exocytic transport pathway are not known. We have therefore used cytochemical and immunocytochemical techniques to study the distribution of virus particles and budding virus in the membranes of the exocytic pathway. In addition, low-temperature incubations were used to investigate the association of virus proteins with the early-secretory-pathway membranes. The results indicate that virus budding begins at the pre-Golgi intermediate compartment and continues in the

* Corresponding author. Mailing address: Department of Biosciences, Division of Biochemistry, Genetics and Cell Biology Programme, University of Helsinki Biocenter, P.O. Box 56 (Viikinkaari 5), 00014 Helsinki University, Finland. Phone: 358-9-708 59048. Fax: 358-9-708 59068. E-mail: Esa.Kuismanen@Helsinki.Fi.

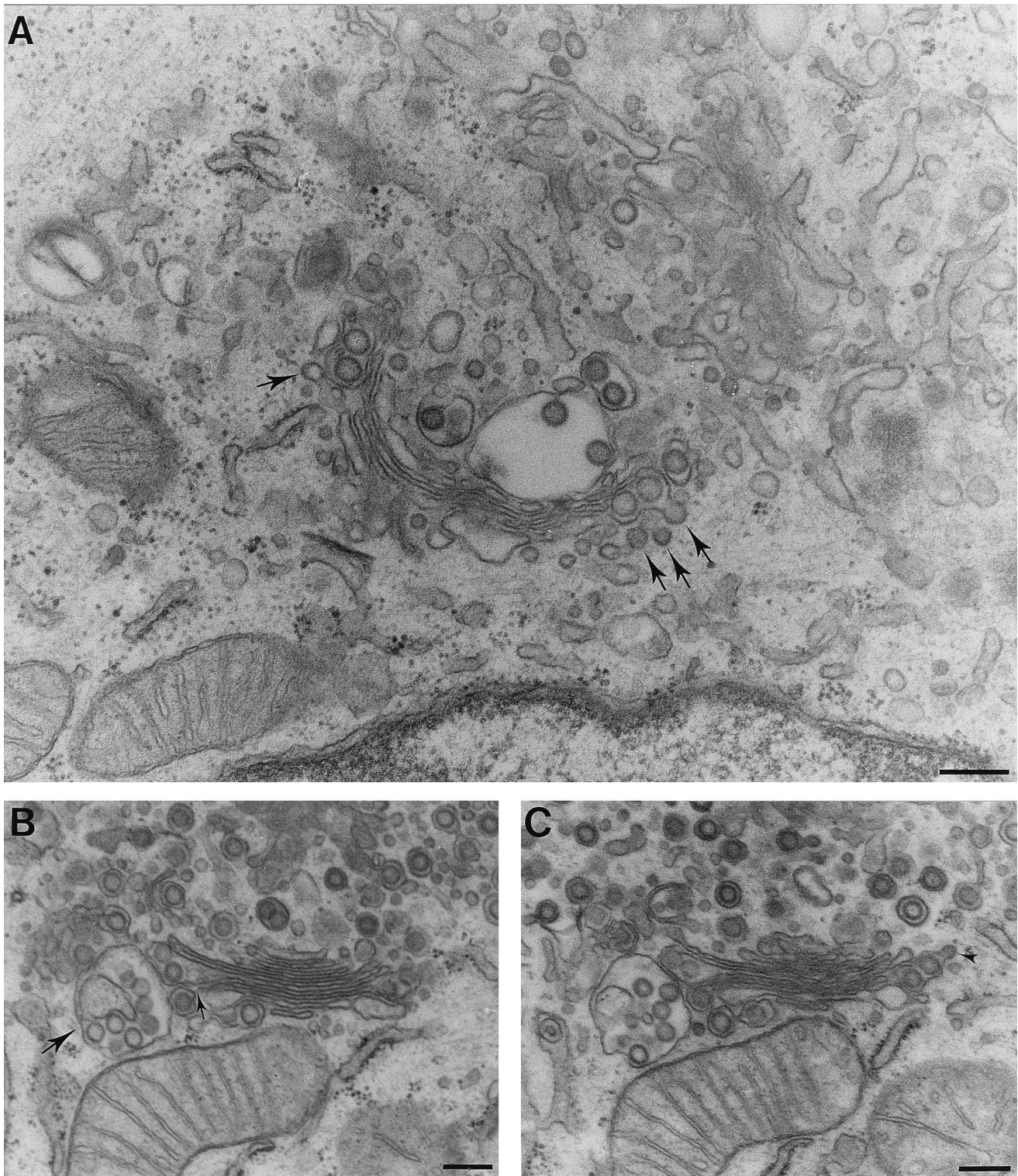


FIG. 1. Electron microscopy of Uukuniemi virus-infected BHK-21 cells. Virus particles are seen in the lumen of the Golgi cisternae and in Golgi-associated vacuoles and vesicles. The virus particles in the stack are present in the dilated rims of the cisternae. The small, approximately 60-nm, vesicles can be seen budding from the cisternae (A, arrows; C, arrowhead). Note that these vesicles are smaller than the virus particles in the lumen of the cisternae. Serial section analysis (B and C) demonstrates that the limiting membrane of large virus-containing vacuoles (B, large arrow) are occasionally continuous with the cisternal membrane (B, small arrow) even in the middle of the stack. Bars, 200 nm.

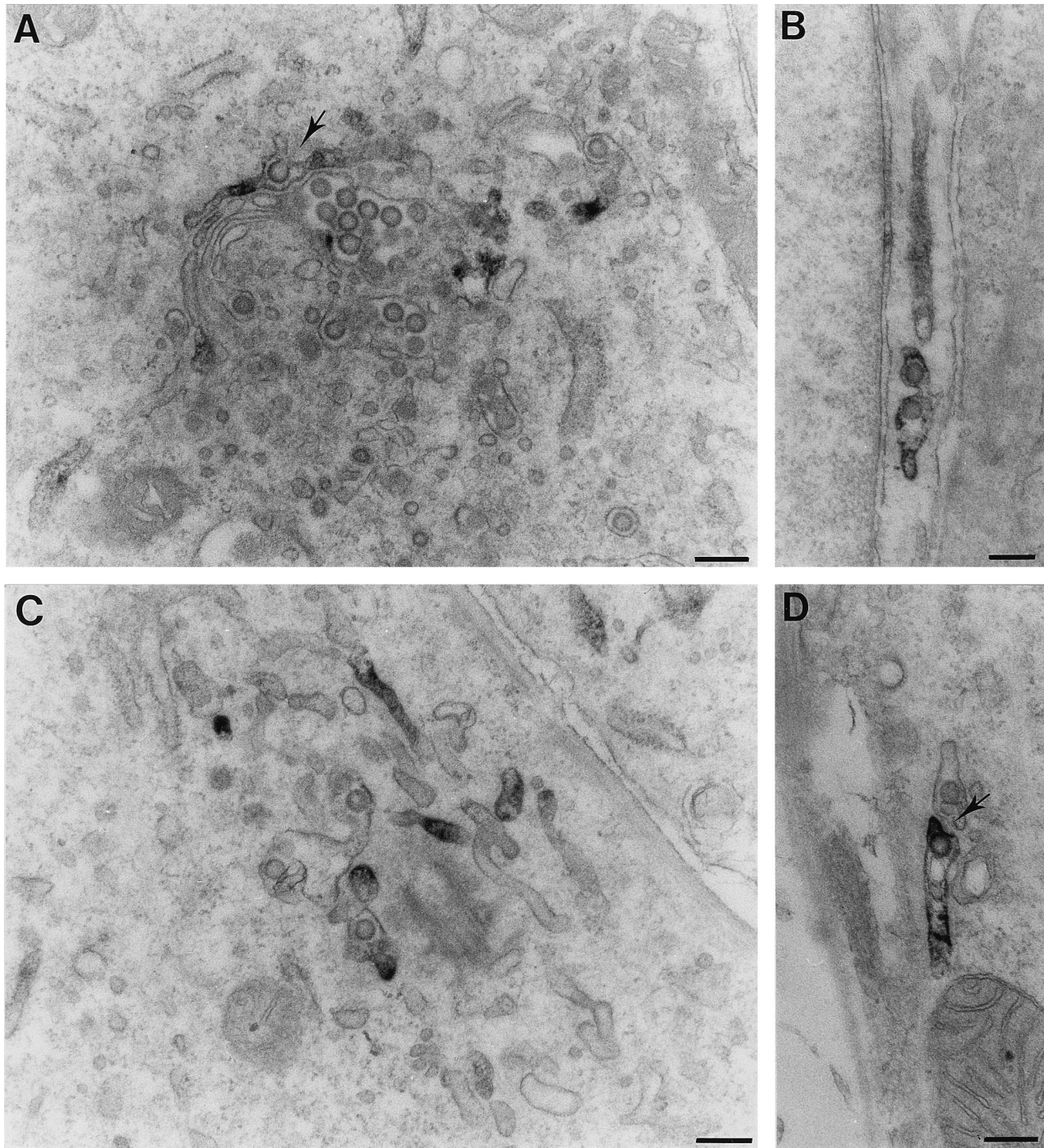


FIG. 2. Colocalization of intermediate compartment marker protein p58 with virus-containing intracellular membranes. BHK-21 cells were fixed 10 h p.i. and processed for immunolabeling as indicated in Materials and Methods. Virus particles can be found in both the perinuclear Golgi and peripheral intermediate compartment membranes labeled with p58. Note the virus budding profiles in the p58-positive *cis* Golgi cisternae of the Golgi stack (A) and in the peripheral tubular elements (D) marked with arrows. Virus particles were consistently found in both the p58-positive and p58-negative parts of the intermediate compartment membranes. Bars, 200 nm.

cisternae of the Golgi stack. Because the putative 60-nm-diameter intra-Golgi transport vesicles are too small to carry the 100- to 120-nm-diameter virus particles, the results raise questions about the intracellular transport mechanism of the virus particles.

MATERIALS AND METHODS

Cell culture and virus infections. Propagation of Uukuniemi stock virus in secondary chicken embryo fibroblasts was done as described previously (8, 32). BHK-21 cells were grown on coverslips to 50 to 70% confluence in minimal essential medium (MEM; Sigma) supplemented with 10% fetal calf serum,

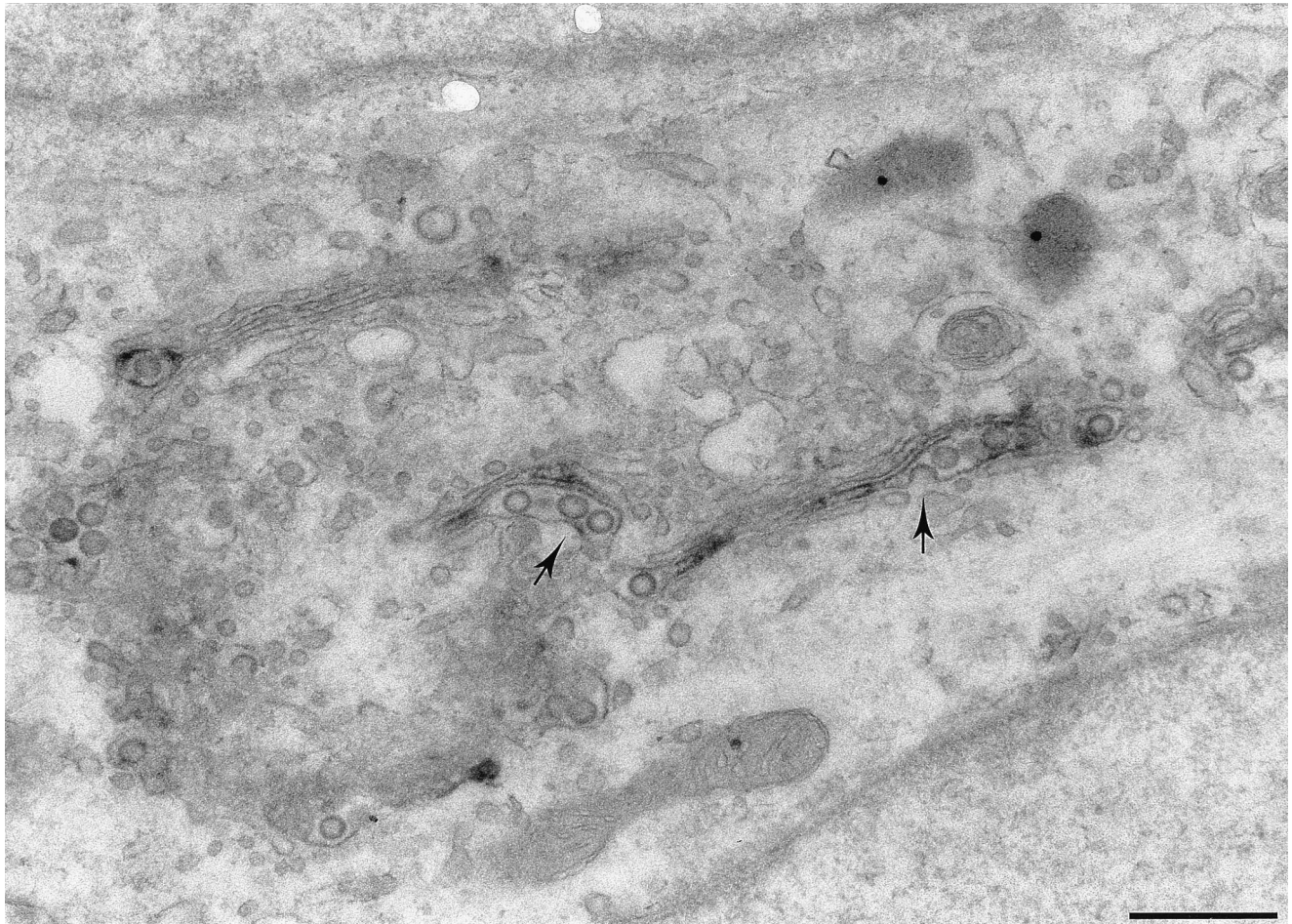


FIG. 3. Budding of Uukuniemi virus in ManII-positive Golgi cisternae. BHK-21 cells were fixed 10 h p.i. and processed for immunolabeling as indicated in Materials and Methods. The arrows mark budding profiles in the ManII-positive Golgi cisternae. Bar, 500 nm.

penicillin (100 IU/ml), and streptomycin (100 mg/ml) and were infected with Uukuniemi virus as described previously (32). Low-temperature incubations of the cells in water baths were carried out in bicarbonate-free MEM supplemented with 20 mM HEPES (pH 7.3) (17).

Immunofluorescence. The cells were fixed for 30 min with 3% paraformaldehyde or 3% paraformaldehyde and 0.08% glutaraldehyde in 0.1 M phosphate buffer (pH 7.2). After permeabilization with 0.05% Triton X-100, the cells were labeled with primary antibodies and fluorochrome-conjugated secondary antibodies as described previously (17). Antibodies used were rabbit antinucleocapsid antibodies and guinea pig anti-G1/G2 antibodies, prepared as described previously (13), and rabbit anti-p58 antibodies (18, 39, 41). The secondary antibodies used were fluorescein isothiocyanate-conjugated rabbit anti-guinea pig immunoglobulin G (IgG) (Dako, Copenhagen, Denmark) and tetramethyl rhodamine isothiocyanate-conjugated swine anti-rabbit IgG (Dako). The samples were viewed with a Zeiss Lab 16 fluorescence microscope using a 100 \times objective. Photography was done with Kodak Tmax-400 ASA film.

Subcellular fractionation. Cell fractionation and gradient centrifugation were carried out essentially as described previously (37). Two 10-cm dishes (Falcon) of subconfluent BHK-21 cells were infected with Uukuniemi virus stock solution as described previously (32). At 7 h postinfection (p.i.) the cells were transferred for 3 h to 15 $^{\circ}$ C in bicarbonate-free MEM (Sigma) buffered with 20 mM HEPES. The cells were then washed with ice-cold phosphate-buffered saline, pH 7.4, and harvested into hypotonic lysis buffer (10 mM Tris, 10 mM KCl, 5 mM MgCl₂ [pH 7.0]). The cells were disrupted by passing the solution 15 times through a 27-gauge needle. The postnuclear supernatant (0.5 ml) was then subjected to flotation analysis by dispersing the sample into 3.5 ml of 70% (wt/wt) sucrose in low-salt buffer (LSB) (50 mM Tris, 25 mM KCl, 5 mM MgCl₂ [pH 7.5]), which was overlaid with 6.5 ml of 55% (wt/wt) sucrose in LSB and 1.5 to 2 ml of 10% (wt/wt) sucrose in LSB. The gradients were centrifuged for 18 h at 38,000 rpm at 4 $^{\circ}$ C in a Beckman ultracentrifuge with an SW41 rotor. Fractions (about 1 ml) were collected from the bottom. The fractions were diluted with LSB containing 0.25 M sucrose, and to pellet the membranes the samples were centrifuged for

90 min with an SW55 rotor at 45,000 rpm at 4 $^{\circ}$ C. The pellets were suspended in LSB and equal aliquots were subjected to sodium dodecyl sulfate-polyacrylamide gel electrophoresis analysis and immunoblotting. Uukuniemi virus nucleocapsid protein was detected with rabbit anti-nucleocapsid antibodies and alkaline phosphatase-conjugated anti-rabbit IgG (Promega).

Electron microscopy. For conventional electron microscopy the cells were fixed for 2 h with 3% paraformaldehyde–2% glutaraldehyde in 0.1 M cacodylate, pH 7.4, at room temperature followed by postfixation with 1% OsO₄ on ice. To localize the nucleocapsid association sites, Uukuniemi virus-infected BHK-21 cells were fixed for 30 min at room temperature with 3% paraformaldehyde–0.08% glutaraldehyde–0.05% saponin in 0.1 M phosphate buffer (pH 7.2). After fixation the cells were washed with DBS buffer (phosphate-buffered saline supplemented with 0.2% bovine serum albumin and 0.05% saponin, pH 7.2) followed by treatment with 0.05 M lysine in DBS buffer to quench free aldehyde groups. The cells were labeled with rabbit antinucleocapsid antibodies and peroxidase-conjugated anti-rabbit F(ab)₂ secondary antibodies (Immunotech, Marseille, France) as described previously (11, 17). For labeling with antibodies to the p58 protein and mannosidase II (ManII), the cells were fixed with the periodate-lysine-paraformaldehyde fixative (3, 23). After development of the peroxidase reaction the samples were postfixated with reduced 1% OsO₄. The samples embedded in LX-112 (Ladd Research Industries, Inc., Burlington, Vt.) were cut horizontally and the sections were viewed in a JEOL JEM EX-1200 electron microscope operated at an acceleration voltage of 60 kV.

RESULTS

Electron microscopy of Uukuniemi virus-infected BHK-21 cells. Previous studies have shown that bunyaviruses mature by budding at intracellular smooth membranes representing the Golgi complex (13, 29, 42). However, morphological analysis of

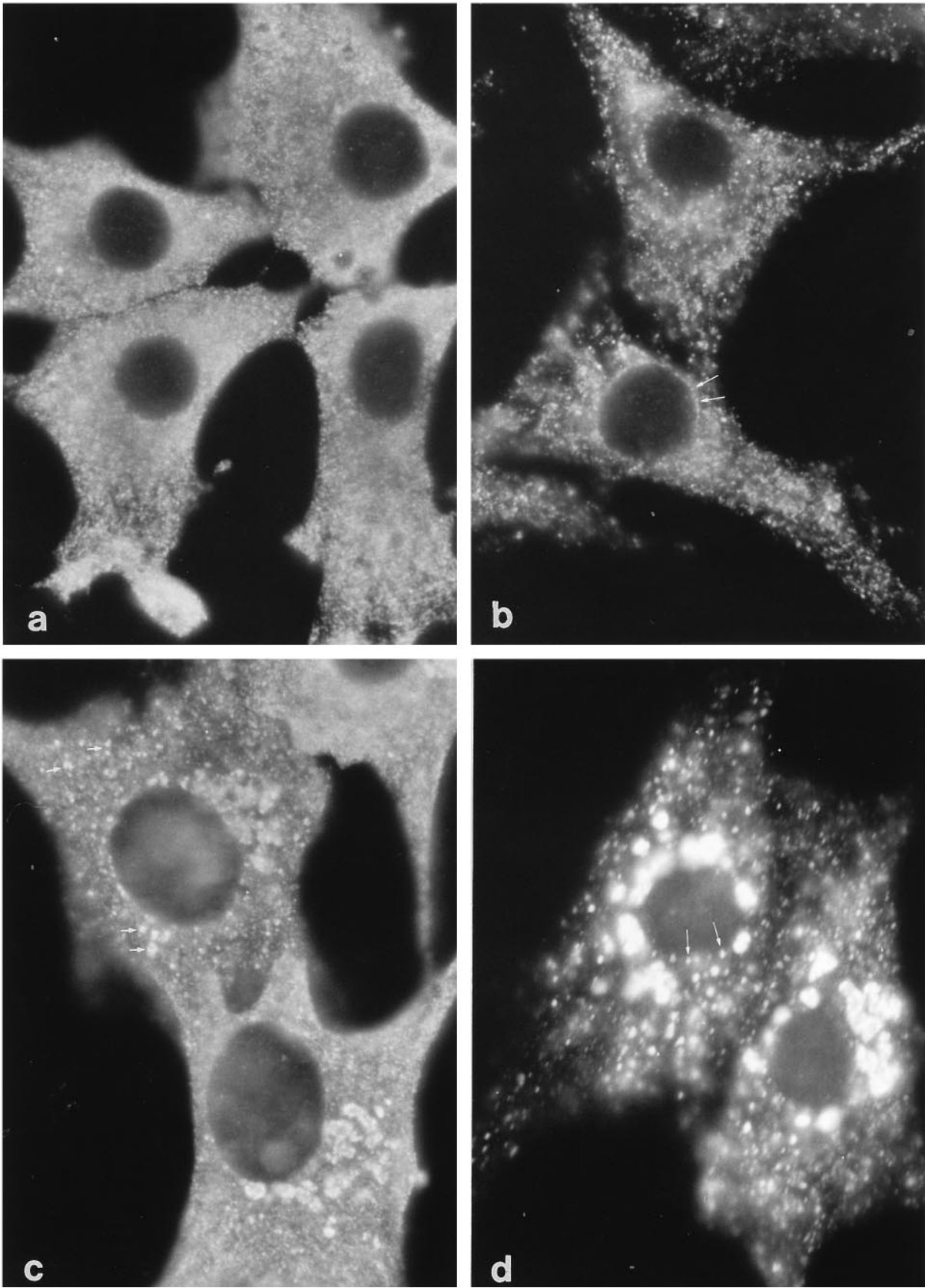


FIG. 4. Association of nucleocapsid with membranes. (a) BHK-21 cells were infected with Uukuniemi virus, fixed with 3% paraformaldehyde-0.08% glutaraldehyde at 7 h p.i., and stained with anti-nucleocapsid antibodies and tetramethyl rhodamine isothiocyanate-conjugated secondary antibodies. (b) Cells were treated from 7 to 7.5 h p.i. with 0.1% saponin on ice, fixed, and stained with nucleocapsid antibodies. Note the absence of perinuclear Golgi-like staining in panels a and b. An apparent association of the label with the nuclear membrane was occasionally detected (b, arrows). (c) Cells were incubated at 15°C from 7 to 10 h p.i. prior to fixation and staining. (d) Cells were incubated at 15°C from 7 to 10 h p.i., treated with 0.1% saponin on ice, fixed, and stained with nucleocapsid antibodies. Note the presence of both peripheral and juxtannuclear nucleocapsid-positive elements in cells incubated at 15°C (c and d, arrows).

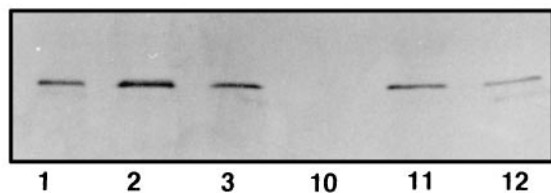


FIG. 5. Association of nucleocapsid with microsomal membranes. Uukuniemi virus-infected cells were incubated at 15°C from 7 to 10 h p.i. Microsomes isolated from the cells were analyzed by flotation in sucrose gradient and immunoblotting with antinucleocapsid antibodies. The presence of the nucleocapsid protein in fractions 11 and 12 demonstrates partial association of the nucleocapsid with floated microsomal membranes.

the exact site of virus maturation has been difficult because bunyaviruses induce a progressive morphological alteration of Golgi membranes resulting in the disappearance of the normal stacked organization of the Golgi complex. However, these fragmented Golgi membranes have been shown to be capable of efficient protein transport and modification (9). Early in the course of infection (8 to 10 h p.i.), relatively intact Golgi complexes can still be found (15). We therefore carried out an analysis by electron microscopy of the distribution of virus particles in the Golgi stacks at 10 h p.i. (Fig. 1). In the Golgi stacks which still retained normal morphology, the virus particles were seen in the lumen of the cisternae throughout the stack (Fig. 1B and C). The virus particles were consistently found in the dilated rims of the cisternae. Occasionally the rims of the cisternae were swollen into large virus-containing vacuoles (Fig. 1B and C and 2A). In the Golgi region the virus particles were also observed in large vesicles and vacuoles on both sides of the stack (Fig. 1 and 2). In addition, virus particles were present in more peripheral sites in the lumens of membranous structures showing variable morphology. The presence of virus particles in all of the cisternae in the Golgi stack indicates that virus budding is not restricted to the medial or the *trans* Golgi membranes. According to previous biochemical analysis, secreted Uukuniemi virus contains terminally glycosylated, protein-bound glycans (14, 31). Since the glycoproteins in virus particles must encounter the glycosyl transferases resident in the *trans* Golgi it is evident that those virus particles seen in the proximal portion of the Golgi stack must be transported to the cell exterior via the *trans* Golgi membranes or their functional equivalent. Electron microscopy of the virus-containing Golgi stacks also demonstrated the presence of approximately 60-nm-diameter vesicles which were seen budding from the cisternae containing lumenal virus (Fig. 1A). Vesicles of similar size have been postulated to function in the vectorial intra-Golgi transport of secreted and membrane glycoproteins (35, 36). It should be noted that Uukuniemi virus particles in the lumens of the cisternae (Fig. 1A) are considerably larger than these vesicles, and therefore it is likely that the cisternae themselves are the vehicles responsible for the vectorial transport of the virus particles.

Analysis of the budding compartment(s). Because the distribution of Uukuniemi virus particles in the Golgi stack suggested that the virus budding might start earlier than previously assumed, we carried out a detailed analysis of the localization of virus particles with compartment-specific markers. We first used immunoperoxidase electron microscopy (IEM) with antibodies to p58 protein, a marker for the intermediate compartment and the *cis* Golgi (39, 41). Uukuniemi virus-infected BHK-21 cells were processed for IEM at 10 h p.i. (Fig. 2), and localization of virus particles, budding virus, and p58 label was monitored. Interestingly, virus particles and

budding profiles were seen in p58-positive *cis* Golgi elements and also in peripheral membranes of the intermediate compartment (Fig. 2). Budding profiles and virus particles were also detected in the p58-positive *cis*-most cisterna of the Golgi stack (Fig. 2A). In addition, the peripheral p58-positive elements with characteristic tubulo-vesicular morphology contained lumenal Uukuniemi virus particles and budding profiles (Fig. 2B to D). Virus particles were consistently detected at both p58-positive and p58-negative regions of the intermediate compartment (Fig. 2C and D). Despite careful examination, no virus particles or budding profiles were observed in the ER membranes, which is in agreement with previous reports on the maturation site of bunyaviruses (25). The role of the Golgi stack in virus budding was studied by using immunoelectron microscopy with antibodies to ManII, a Golgi stack enzyme (44). In agreement with previous reports, virus particles and budding profiles were observed in the ManII-positive cisternae in the Golgi stack (Fig. 3). Taken together, these results indicate that the budding of Uukuniemi virus begins in the pre-Golgi intermediate compartment and continues in the Golgi stack. Therefore, the region of virus maturation in the exocytic pathway is more widely distributed than previously assumed.

Association of the nucleocapsid with the intermediate compartment. At 5 to 7 h p.i. the virus nucleocapsid is evenly distributed throughout the cytoplasm of BHK-21 cells. Later, at 8 to 10 h p.i., the nucleocapsid concentrates in the Golgi region (15). Although the first site of nucleocapsid association should reside in the intermediate compartment, since the virus budding is observed there, the binding of nucleocapsid to the intermediate compartment is difficult to monitor because the cytosolic pool of the nucleocapsid masks detection. Therefore, to study the association of the nucleocapsid with the intermediate compartment, we used incubations at reduced temperature (15°C), which amplifies the intermediate compartment membranes due to an arrest of membrane traffic to the Golgi stack. Furthermore, unattached virus glycoproteins accumulate in the intermediate compartment at 15°C (17, 38, 40), which facilitates detection of the nucleocapsid binding with these membranes. BHK-21 cells were infected with Uukuniemi virus and incubated for 7 h at 37°C. Control cells, fixed at 7 h p.i., showed negligible accumulation of the nucleocapsid in the juxtannuclear Golgi region (Fig. 4a). However, when the cells were incubated at 15°C from 7 to 10 h p.i., the nucleocapsid accumulated in the Golgi region in over 90% of the cells (Fig. 4c). Interestingly, in these cells the nucleocapsid also accumulated in peripheral elements distributed throughout the cytoplasm (Fig. 4c). Membrane association of the nucleocapsid was further demonstrated by treatment of the cells with 0.1% saponin on ice before fixation (3% paraformaldehyde and 0.08% glutaraldehyde) and processing for immunofluorescence. This treatment removed the bulk of the free nucleocapsid in the cell cytoplasm, revealing those associated with membrane elements (Fig. 4b and d). Saponin-treated control cells fixed at 7 h p.i. (Fig. 4b) showed negligible association of the nucleocapsid to the membranes in the Golgi region. However, in cells incubated at 15°C, saponin treatment revealed a strong accumulation of the nucleocapsid in membranes in the Golgi region (Fig. 4d). Furthermore, labeling of the peripheral elements became clearly visible in these cells (Fig. 4d). At a later time p.i. (10 h), this nucleocapsid association with peripheral elements was also seen in cells incubated at 37°C and fixed after saponin treatment (data not shown). Association of the nucleocapsid with membranes was further demonstrated by cell fractionation and sucrose gradient centrifugation. Uukuniemi virus-infected BHK-21 cells were incubated at 15°C from 7 to 10 h p.i. The cells were disrupted, and postnuclear supernatant

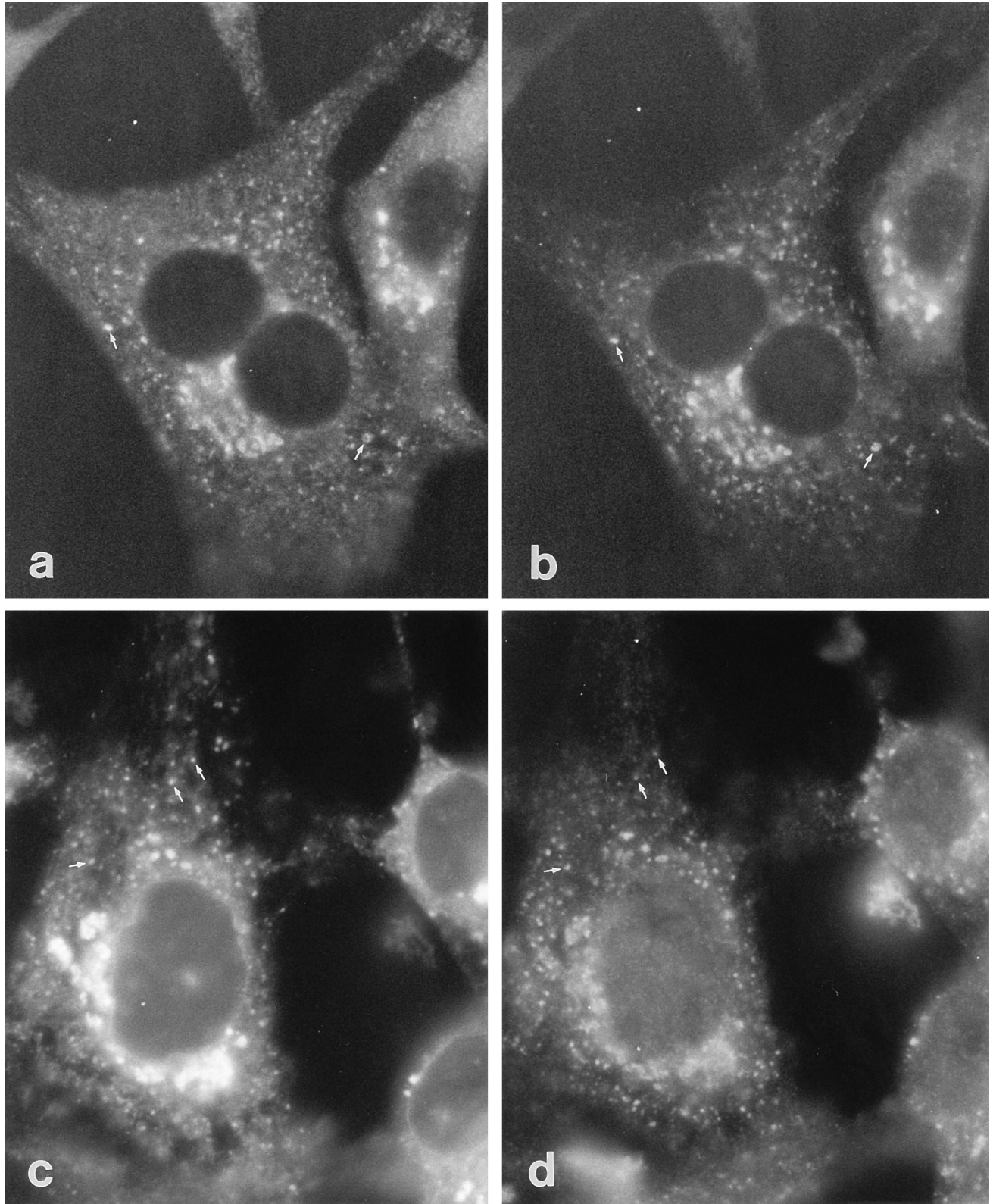


FIG. 6. Association of nucleocapsid with peripheral and juxtannuclear glycoprotein-positive elements at 15°C. Uukuniemi virus-infected cells were incubated at 15°C from 7 to 10 h p.i., fixed with 3% paraformaldehyde, and stained with antinucleocapsid antibodies and anti-G1/G2 antibodies (a and b, respectively). Colocalization of the proteins both at the juxtannuclear Golgi region and at peripheral sites (arrows) is evident. (c and d) Double localization of the virus glycoproteins and p58, a pre- and *cis* Golgi marker, in cells incubated at 15°C. The cells incubated from 7 to 10 h p.i. at 15°C were labeled with guinea pig anti-G1/G2 antiserum (c). Staining of the same cells with rabbit anti-p58 antibodies (d) demonstrates that during incubation at reduced temperature the virus glycoproteins accumulate in juxtannuclear and peripheral (arrows) p58-positive elements.

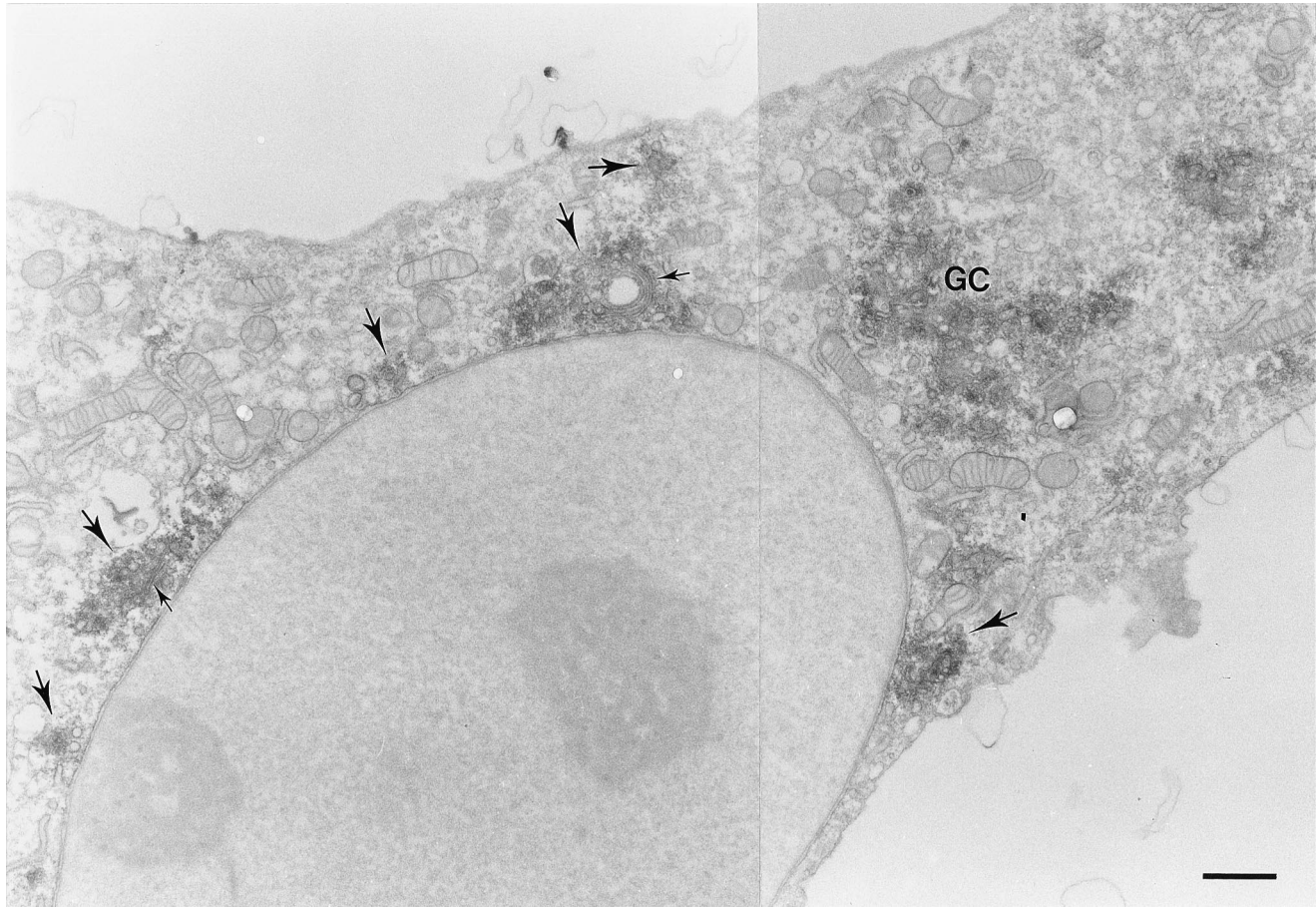


FIG. 7. IEM of Uukuniemi virus-infected cells incubated at 15°C. Nucleocapsid is found associated with juxtannuclear Golgi elements (GC) and 15°C intermediates distributed throughout the cytoplasm (large arrows). The morphology of these elements varies from small vesicular clusters to larger aggregates of membranes occasionally showing cisternal organization (small arrows). Cytoplasmic vesicular clusters can be seen in association with the ER and nuclear membrane, and even close to the plasma membrane. Note the staining apparently associated with the outer nuclear membrane. This staining is most prominent under the labeled 15°C intermediates. Bar, 1 μ m.

was subjected to flotation analysis in a sucrose gradient. The microsome fraction, floated to the 55%-10% sucrose interface, contained Uukuniemi virus nucleocapsid protein (Fig. 5, fractions 11 and 12), indicating that a quantity of nucleocapsid was bound to microsomal membranes during low-temperature treatment of the cells.

To further characterize the membranes with which the nucleocapsid associates during the 15°C incubation, we used double-label immunofluorescence. Uukuniemi virus-infected cells were incubated at 15°C from 7 to 10 h p.i., fixed, and double labeled with rabbit antinucleocapsid antibodies (Fig. 6a) and with guinea pig antiglycoprotein antibodies (Figure 6b). The nucleocapsid and the glycoproteins were found to colocalize both in the juxtannuclear Golgi region and in vesicular elements distributed throughout the cytoplasm (Fig. 6a and b). Double labeling with the pre- and *cis* Golgi marker p58 (39, 41) showed colocalization of the p58 and the virus glycoproteins both in the juxtannuclear region and in the peripheral elements (Fig. 6c and d). This further indicates that the structural proteins of Uukuniemi virus accumulate in the pre-Golgi intermediate compartment in cells incubated at 15°C.

Immunoelectron microscopy analysis of the nucleocapsid binding membranes. Since the nucleocapsid associated with membranes showing a characteristic distribution of the intermediate compartment, we analyzed the morphological features

of these membranes by IEM. To arrest the transport of virus glycoproteins at the intermediate compartment, virus-infected BHK-21 cells were incubated from 7 to 10 h p.i. at 15°C and then prepared for IEM by using antinucleocapsid antibodies (Fig. 7 and 8). The overall distribution of the labeled membrane elements was similar to that observed in immunofluorescence experiments (Fig. 4c). Nucleocapsid was seen associated with membranes in the Golgi region and with membranes of the peripheral intermediate compartment showing variable morphology (Fig. 7). Labeled membranes in the Golgi region consisted of vacuoles, clusters of vesicles, and elements with cisternal morphology. The nucleocapsid-positive vacuoles and cisternal elements frequently contained virus particles in their lumens. Outside the Golgi region the labeled structures consisted of vacuoles, tubules, and clusters of vesicles. Interestingly, some peripheral elements also contained small stacks of cisternal membranes which occasionally had a circular appearance (Fig. 7). Detailed analysis of the peripheral labeled membranes (Fig. 8) demonstrated that the nucleocapsid is associated with tubulo-vesicular elements resembling in morphology the peripheral intermediate compartment (38, 41). These elements were surrounded by ER membranes which occasionally showed labeling (Fig. 8C). Frequently, vacuoles associated with the tubulo-vesicular structures were seen to contain virus particles (Fig. 8C and D) or even budding virus (Fig. 8D).

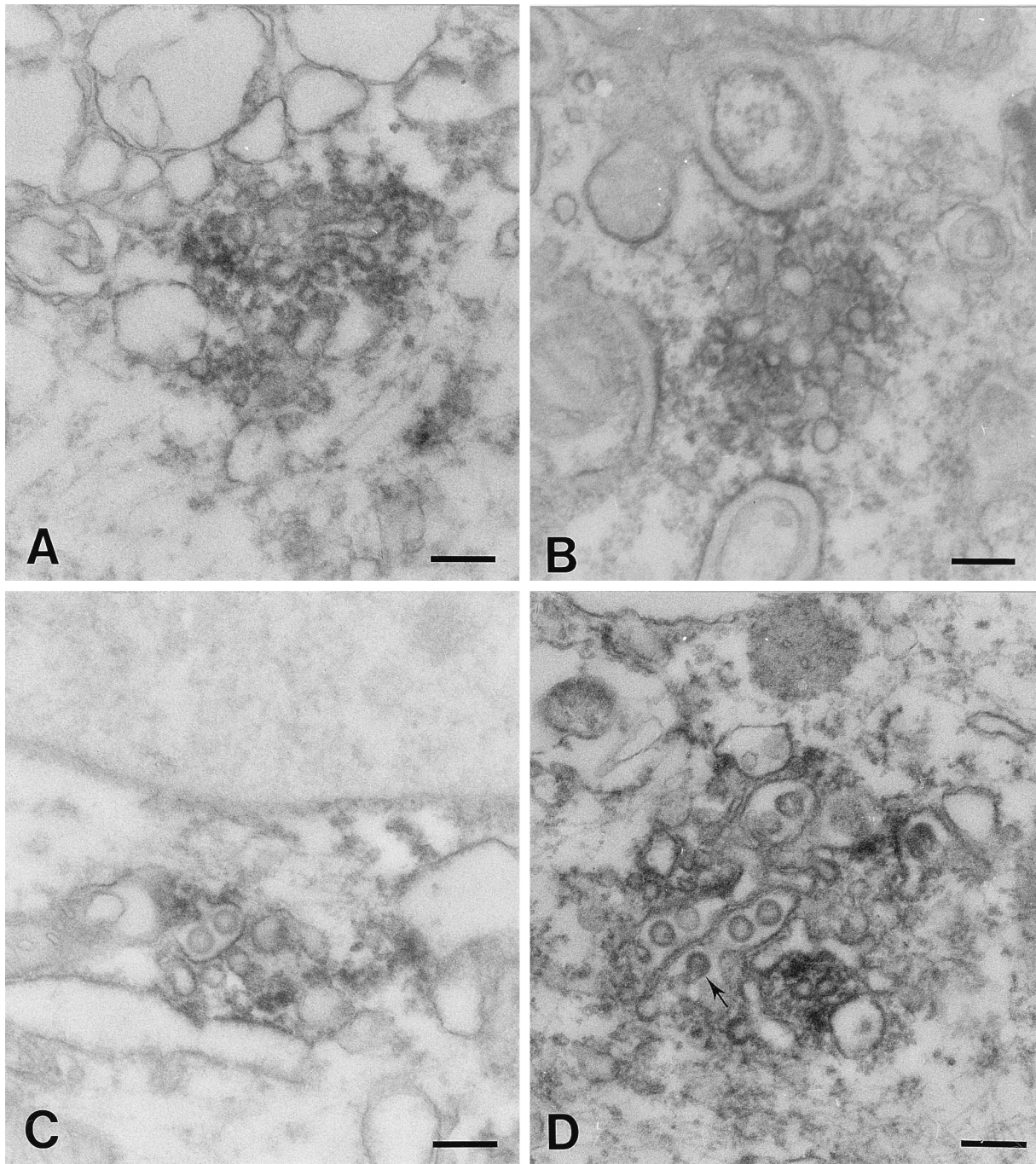


FIG. 8. Morphology of nucleocapsid-positive 15°C intermediates. Nucleocapsid label is associated with clusters of cytoplasmic vesicles, vacuoles, and tubules. The vacuoles in these elements frequently contain virus particles (C and D) and budding virus (D, arrow). Bars, 200 nm.

These results suggest that the first site of nucleocapsid binding and virus budding resides in the pre-Golgi intermediate compartment.

DISCUSSION

The results of the present study demonstrate that the budding of Uukuniemi virus, a bunyavirus, can occur as early as in the pre-Golgi intermediate compartment as well as in the cisternae of the Golgi stack. Immunoelectron microscopy using

p58 protein as a compartment-specific marker clearly showed that Uukuniemi virus particles and budding virus can be found in both peripherally and centrally localized elements of the intermediate compartment. In agreement with previous studies, the virus budding was also observed in the Golgi stack marked by the Golgi enzyme ManII. The results showing budding in the p58-positive membranes were unexpected since it had been assumed previously that bunyaviruses mature exclusively in the Golgi stack or even in the *trans* Golgi membranes (10, 25). Based on the present results it is not possible to

evaluate how much of the budding occurs in the intermediate compartment compared to the stack. However, it was not difficult to detect virus particles in the membranes of the intermediate compartment. This suggests that a considerable amount of virus formation takes place in these membranes.

There are several possible mechanisms which could explain the determination of the site of virus maturation. One obvious prerequisite is the accumulation of the structural components at the budding site. It is evident that the structural components of a virus have to reach a critical concentration in the budding compartment. In the case of Uukuniemi virus the concentration of properly folded glycoproteins in the ER may be too low to promote virus formation. Interestingly, accumulation of the glycoproteins of Punta Toro virus, another bunyavirus, to the ER by brefeldin A treatment results in virus budding in the ER (4). Also, Uukuniemi virus nucleocapsid associates with virus glycoproteins when they are accumulated in the ER membranes by tunicamycin treatment of the cells (15). Recently, it has been shown that accumulation of the bunyavirus glycoproteins in the Golgi stack was mediated by the targeting signal in one of the envelope glycoproteins (4, 5, 26, 34). According to a simple view, the budding mechanism would include a signal-mediated retardation and accumulation of the glycoproteins in the Golgi and subsequent association of the nucleocapsid with the cytosolic domains of the glycoproteins. The present results suggest that additional mechanisms are involved in the budding process. It is possible that the critical budding concentration of the virus glycoproteins has already been reached when they enter the intermediate compartment. Indeed, there is evidence that transported proteins are concentrated considerably on their exit from the ER (1, 28). The observed enhanced binding of the nucleocapsid protein to the intermediate compartment during 15°C incubations suggests that concentration of the glycoproteins is also a factor in the budding in the pre-Golgi membranes. In conclusion, the accumulation of Uukuniemi virus glycoproteins in the Golgi stack due to the targeting signals does not seem to be the only determinant in the selection of the budding site. The same appears to apply for mouse hepatitis coronavirus (MHV), another intracellularly maturing virus. The membrane protein M of MHV is targeted to the *trans* Golgi, although the virus budding occurs in the intermediate compartment (12). In contrast, the glycoprotein M of avian coronavirus infectious bronchitis virus is targeted to the intermediate compartment and the *cis* Golgi, where its budding also takes place (21, 22).

How the assembly of Uukuniemi virus envelope-spike complexes takes place is not known exactly. Studies on the glycoprotein complexes in the virus particles indicate that the spikes are formed from oligomers of glycoprotein homodimers (33). It is possible that the requirements for oligomerization of the homodimers are first met in the intermediate compartment. The glycoprotein oligomers would then support the binding of the nucleocapsid to the membranes. Immunocytochemical experiments with antibodies recognizing the cytosolic part of the G1 glycoprotein suggest that the cytosolic domain is hidden in the ER and that its conformation changes downstream in the transport pathway (17a). Therefore, the exposure or conformational change in the cytosolic portions of the glycoproteins may serve as a control switch for the nucleocapsid binding and virus budding. Understanding these processes requires further studies on the early steps of maturation of the virus glycoproteins and detailed studies on the molecular interactions of the structural components of Uukuniemi virus particles.

The results of the present study suggest that important information on the organization of the secretory pathway can be obtained by using the Uukuniemi virus as a model. In partic-

ular, the observed distribution of virus particles and budding profiles raises questions about the mechanism of transport in the early secretory pathway and in the Golgi stack. The virus particles secreted from infected cells contain only terminally glycosylated G1 glycoprotein (14). For those particles which were formed in the early secretory pathway, the terminal processing of protein-bound glycans, e.g., sialylation, may therefore occur in the envelope of the virus. This would indicate that the virus particles formed in the intermediate compartment or in the *cis* Golgi are transported through the functional Golgi stack to the *trans* Golgi before externalization. Alternatively, mature glycoproteins may be recycled to the budding site as suggested for MHV (12).

The size of Uukuniemi virus particles (approximately 100 to 120 nm in diameter) excludes the possibility that the transport occurs in the 60-nm-diameter vesicles postulated to function as carriers between the compartments of the exocytic pathway. The role of such vesicles in the vectorial intra-Golgi traffic has been questioned (2, 6, 7, 20, 27, 40, 45). The results of the present study suggest that the intra-Golgi transport of Uukuniemi virus particles takes place in the dilated portions of the Golgi cisternae. This transport pathway of the virus particles through the Golgi resembles the morphological pathway observed in the case of maturation and secretion of collagen granules (19, 24). Also, similar distribution within the Golgi has been reported for the hepatic apolipoprotein E, which localizes in saccular distensions of the Golgi cisternae (7). For the transport of virus particles through the Golgi, another possible mechanism is the budding of virus-containing vacuoles from the dilated rims of the Golgi cisternae. If this is the case, the Golgi-derived vacuoles have to undergo maturation and achieve functional characteristics of the *trans* Golgi, since the glycans in the virus-bound G1 glycoprotein undergo terminal processing, including sialylation (14). These two mechanisms of transport are not necessarily mutually exclusive. It is possible that early in the infection the transport of virus particles occurs in the lumen of the intermediate compartment and maturing Golgi cisternae and later, when the stacked organization of the Golgi is lost, in maturing vacuoles which achieve the functional characteristics of successive compartments of the Golgi complex.

ACKNOWLEDGMENTS

We thank Carolyn Machamer and R. Rönholm for helpful comments and critical reading of the manuscript. Skillful technical assistance by Mervi Lindman and Anne Makkonen is gratefully acknowledged. We thank J. Saraste for the antibodies to p58 protein and M. G. Farquhar and K. Moremen for the ManII antibodies.

The study was supported by research grants to E.K. and S.K. from the Academy of Finland.

REFERENCES

- Balch, W. E., J. M. McCaffery, H. Plutner, and M. G. Farquhar. 1994. Vesicular stomatitis virus glycoprotein is sorted and concentrated during export from the endoplasmic reticulum. *Cell* 76:841-852.
- Becker, B., B. Bölinger, and M. Melkonian. 1995. Anterograde transport of algal scales through the Golgi complex is not mediated by vesicles. *Trends Cell Biol.* 5:305-307.
- Brown, W. J., and M. G. Farquhar. 1989. Immunoperoxidase method for the localization of antigens in cultured cells and tissue by electron microscopy. *Methods Cell Biol.* 31:554-569.
- Chen, S.-Y., Y. Matsuoka, and R. W. Compans. 1991. Assembly and polarized release of Punta Toro virus and effects of brefeldin A. *J. Virol.* 65:1427-1439.
- Chen, S.-Y., and R. W. Compans. 1991. Oligomerization, transport, and Golgi retention of Punta Toro virus glycoproteins. *J. Virol.* 65:5902-5909.
- Cole, N. B., N. Sciaky, A. Marotta, J. Song, and J. Lippincott-Schwartz. 1996. Golgi dispersal during microtubule disruption: regeneration of Golgi stacks at peripheral endoplasmic reticulum exit sites. *Mol. Biol. Cell* 7:631-650.

7. **Dahan, S., J. P. Ahluwalia, L. Wong, B. L. Posner, and J. J. N. Bergeron.** 1994. Concentration of intracellular hepatic apolipoprotein E in Golgi apparatus saccular distensions and endosomes. *J. Cell Biol.* **127**:1859–1869.
8. **Gahmberg, N.** 1984. Characterization of two recombination-complementation groups of Uukuniemi virus temperature-sensitive mutants. *J. Gen. Virol.* **65**:1079–1090.
9. **Gahmberg, N., R. F. Pettersson, and L. Kääriäinen.** 1986. Efficient transport of Semliki Forest virus glycoproteins through a Golgi complex morphologically altered by Uukuniemi virus glycoproteins. *EMBO J.* **5**:3111–3118.
10. **Griffiths, G., and P. Rottier.** 1992. Cell biology of viruses that assemble along the biosynthetic pathway. *Semin. Cell Biol.* **3**:367–381.
11. **Jääntti, J., and E. Kuismanen.** 1993. Effect of caffeine and reduced temperature (20°C) on the organization of the pre-Golgi and the Golgi stack membranes. *J. Cell Biol.* **120**:1321–1335.
12. **Klumperman, J., J. Krijnse Locker, A. Meijer, M. C. Horzinek, H. J. Geuze, and P. J. M. Rottier.** 1994. Coronavirus M proteins accumulate in the Golgi complex beyond the site of virion budding. *J. Virol.* **68**:6523–6534.
13. **Kuismanen, E., K. Hedman, J. Saraste, and R. F. Pettersson.** 1982. Uukuniemi virus maturation: accumulation of virus particles and viral antigens in the Golgi complex. *Mol. Cell. Biol.* **2**:1444–1458.
14. **Kuismanen, E.** 1984. Posttranslational processing of Uukuniemi virus glycoproteins G1 and G2. *J. Virol.* **51**:806–812.
15. **Kuismanen, E., B. Bång, M. Hurme, and R. F. Pettersson.** 1984. Uukuniemi virus maturation: immunofluorescence microscopy with monoclonal glycoprotein-specific antibodies. *J. Virol.* **51**:137–146.
16. **Kuismanen, E., J. Saraste, and R. F. Pettersson.** 1985. Effect of monensin on the assembly of Uukuniemi virus in the Golgi complex. *J. Virol.* **55**:813–822.
17. **Kuismanen, E., and J. Saraste.** 1989. Low temperature induced transport blocks as tools to manipulate membrane traffic. *Methods Cell Biol.* **32B**:257–274.
- 17a. **Kuismanen, E.** Unpublished observation.
18. **Lahtinen, U., B. Dahllöf, and J. Saraste.** 1992. Characterization of a 58 kDa cis-Golgi protein in pancreatic exocrine cells. *J. Cell Sci.* **103**:321–333.
19. **Leblond, C. P.** 1989. Synthesis and secretion of collagen by cells of connective tissue, bone, and dentin. *Anat. Rec.* **224**:123–138.
20. **Lippincott-Schwartz, J.** 1993. Bidirectional membrane traffic between the endoplasmic reticulum and the Golgi apparatus. *Trends Cell Biol.* **3**:81–88.
21. **Machamer, C. E., and J. K. Rose.** 1987. A specific transmembrane domain of a coronavirus E1 glycoprotein is required for its retention in the Golgi region. *J. Cell Biol.* **105**:1205–1214.
22. **Machamer, C. E., S. A. Mentone, J. K. Rose, and M. G. Farquhar.** 1990. The E1 glycoprotein of an avian coronavirus is targeted to the cis-Golgi complex. *Proc. Natl. Acad. Sci. USA* **87**:6944–6948.
23. **MacLean, M., and P. K. Nakane.** 1974. Periodate-lysine-paraformaldehyde fixative. A new fixative for immunoelectron microscopy. *J. Histochem. Cytochem.* **22**:1077–1083.
24. **Marchi, F., and C. P. Leblond.** 1984. Radioautographic characterization of successive compartments along the rough endoplasmic reticulum-Golgi pathway of collagen precursors in foot pad fibroblasts of 3H-proline-injected rats. *J. Cell Biol.* **98**:1705–1709.
25. **Matsuoka, Y., S. Y. Chen, and R. W. Compans.** 1991. Bunyavirus protein transport and assembly. *Curr. Top. Microbiol. Immunol.* **169**:161–179.
26. **Melin, L., R. Persson, A. Andersson, A. Bergström, R. Rönnholm, and R. F. Pettersson.** 1995. The membrane glycoprotein of Uukuniemi virus contains a signal for localization to the Golgi complex. *Virus Res.* **36**:49–66.
27. **Mellman, I., and K. Simons.** 1992. The Golgi complex: in vitro veritas? *Cell* **68**:829–840.
28. **Mizuno, M., and S. J. Singer.** 1993. A soluble secretory protein is first concentrated in the endoplasmic reticulum before transfer to the Golgi apparatus. *Proc. Natl. Acad. Sci. USA* **90**:5732–5736.
29. **Murphy, F. A., A. K. Harrison, and S. G. Whitfield.** 1973. Bunyaviridae: morphologic and morphogenetic similarities of bunyamwera serologic supergroup viruses and several other arthropod borne viruses. *Intervirology* **1**:297–316.
30. **Persson, R., and R. F. Pettersson.** 1991. Formation and intracellular transport of a heterodimeric viral spike protein complex. *J. Cell Biol.* **112**:257–266.
31. **Pesonen, M., E. Kuismanen, and R. F. Pettersson.** 1982. Monosaccharide sequence of protein-bound glycans of Uukuniemi virus. *J. Virol.* **41**:390–400.
32. **Pettersson, R. F., and L. Kääriäinen.** 1973. The ribonucleic acids of Uukuniemi virus, a non-cubical tick-borne arbovirus. *Virology* **56**:608–619.
33. **Rönkä, H., H. Hilden, P., C.-H. von Bonsdorff, and E. Kuismanen.** 1995. Homodimeric association of the spike glycoproteins of Uukuniemi virus. *Virology* **211**:241–250.
34. **Rönnholm, R.** 1992. Localization to the Golgi complex of Uukuniemi virus glycoproteins G1 and G2 expressed from cloned cDNAs. *J. Virol.* **66**:4525–4531.
35. **Rothman, J. E., and L. Orci.** 1992. Molecular dissection of the secretory pathway. *Nature* **355**:409–415.
36. **Rothman, J. E.** 1994. Mechanisms of intracellular protein transport. *Nature* **372**:555–563.
37. **Sanderson, C. M., N. L. McQueen, and D. P. Nayak.** 1993. Sendai virus assembly: M protein binds to viral glycoproteins in transit through the secretory pathway. *J. Virol.* **67**:651–663.
38. **Saraste, J., and E. Kuismanen.** 1984. Pre- and post-Golgi vacuoles operate in the transport of Semliki Forest virus membrane glycoproteins to the cell surface. *Cell* **38**:535–549.
39. **Saraste, J., G. E. Palade, and M. G. Farquhar.** 1987. Antibodies to rat pancreas Golgi subfractions: identification of a 58-kD cis-Golgi protein. *J. Cell Biol.* **105**:2021–2030.
40. **Saraste, J., and E. Kuismanen.** 1992. Pathways of protein sorting and membrane traffic between the rough endoplasmic reticulum and the Golgi complex. *Semin. Cell Biol.* **3**:343–355.
41. **Saraste, J., and K. Svensson.** 1991. Distribution of intermediate elements operating in ER to Golgi transport. *J. Cell Sci.* **100**:415–430.
42. **Smith, J. F., and D. Y. Pifat.** 1982. Morphogenesis of sandfly fever viruses (Bunyaviridae family). *Virology* **121**:61–81.
43. **Umanen, I., P. Seppälä, and R. F. Pettersson.** 1981. In vitro translation of Uukuniemi virus-specific RNAs: identification of a nonstructural protein and a precursor to the membrane glycoproteins. *J. Virol.* **37**:72–79.
44. **Velasco, A., L. Hendrics, K. W. Moremen, D. R. P. Tulsiani, O. Touster, and M. G. Farquhar.** 1993. Cell-type dependent variations in the subcellular distribution of α -mannosidase I and II. *J. Cell Biol.* **122**:39–51.
45. **Weidman, P. J.** 1995. Anterograde transport through the Golgi complex: do Golgi tubules hold the key? *Trends Cell Biol.* **5**:302–305.